

## SLAG MONITORING SYSTEM FOR COMBUSTION CHAMBERS OF STEAM BOILERS

J. Taler<sup>1</sup> and D. Taler<sup>2</sup>

<sup>1</sup> Department of Power Plant Machinery, Institute of Process and Power Engineering, Cracow University of Technology,  
Al. Jana Pawła II 37, 31-864 Cracow, Poland  
e-mail: [taler@ss5.mech.pk.edu.pl](mailto:taler@ss5.mech.pk.edu.pl)

<sup>2</sup> Department of Power Plant Installations, Faculty of Mechanical Engineering And Robotics, Cracow University of Science and Technology,  
Al. Mickiewicza 30, Paw. B-3, 30-059 Cracow, Poland,  
e-mail: [taler@imir.agh.edu.pl](mailto:taler@imir.agh.edu.pl)

### ABSTRACT

The computer based boiler performance system, presented in this paper, has been developed to provide a direct and quantitative assessment of furnace and convective surface cleanliness. Temperature, pressure and flow measurements and gas analysis data are used to perform heat transfer analysis in the boiler furnace and evaporator. Power boiler efficiency is calculated using an indirect method. The on-line calculation of the exit flue gas temperature in a combustion chamber allows for an on-line heat flow rate determination, which is transferred to the boiler evaporator. Based on the energy balance for the boiler evaporator, the superheated steam mass flow rate is calculated taking into the account water flow rate in attemperators. Comparing the calculated and the measured superheated steam mass flow rate, the effectiveness of the combustion chamber waterwalls is determined in an on-line mode. Sootblower sequencing can be optimized based on actual cleaning requirements rather than on fixed time cycles contributing to lowering of the medium usage in soot blowers and increasing of the water-wall lifetime.

### INTRODUCTION

When coal is burned, a relatively small portion of the ash will cause deposition problems. Due to the differences in deposition mechanisms involved, two types of high temperature ash deposition have been defined as slagging and fouling (Littler, 1991 and Stultz, 1992). Slagging and fouling conditions are critical factors influencing reliability and availability on a coal-fired utility boiler. However, boiler surface deposits have been, traditionally, one of the most difficult operating variables to quantify. Sootblowers are the primary means of dealing directly with furnace wall slagging and convection pass fouling. With traditional methods, operators often are unable to detect the critical build-up of deposits in specific heating surfaces of the boiler. Clyde Bergemann has recently developed a strain-gauge based measurement system for slag deposits (Bergemann, 2004). The system uses strain gauges to measure loads on the rods that suspend the pendant steam

superheaters. The increased weight due to the build up of deposits causes the recorded strain to increase.

Deposits on heat transfer surfaces lead to a reduction in heat flux to the waterside. Local slagging and fouling at a particular location can be detected by heat flux measurements using the heat flux tubes (Taler and Taler, 2007; Taler 2007). In this paper, a system for monitoring the build-up of ash deposits in boiler furnaces and steam superheaters is presented. Power boiler efficiency is calculated using an indirect method. Based on the power boiler energy balance, the fuel mass flow rate  $\dot{m}_F$  is then calculated. The on-line calculation of a combustion chamber allows for an on-line heat flow rate determination, which is transferred to the power boiler evaporator. Based on the energy balance for the power boiler evaporator, the superheated steam mass flow rate is calculated taking into the account water flow rate in attemperators. Comparing the calculated and the measured superheated steam mass flow rate the effectiveness of combustion chamber waterwalls is determined in an on-line mode. Degrees of fouling of the furnace walls  $\zeta_f$  and superheaters  $\zeta_{sup}$  are also determined based on the measurement data. The on-line measurements of ash deposits can be used to guide sootblower operations in a combustion chamber and steam superheaters. Thus, the developed slag monitoring system contributes contributed to lowering of the medium usage in soot blowers and increasing of the water-wall lifetime.

### MONITORING OF THERMAL-HYDRAULIC OPERATING CONDITIONS

In the following, the determination of boiler efficiency, fuel and live steam mass flows, and effectiveness of combustion chamber waterwalls will be discussed in detail. When coal is burned, a relatively small portion of the ash will cause deposition problems. Due to the differences in deposition mechanisms involved, two types of high temperature ash deposition have been defined as slagging and fouling. Slagging is the formation of molten, partially fused deposits on furnace walls and other surfaces exposed to radiant heat. Fouling is defined as the formation of high temperature bonded deposits on convection heat absorbing

surfaces, such as superheaters and reheaters, that are not exposed to radiant heat (Littler, 1991; Stultz and Kitto, 1993). Typical indications of surface fouling appear to the operator indirectly in the form of high steam and flue gas temperatures, large attemperation flows and draft losses. If the furnace walls are slagged, the result is low mass flow of saturated steam from the evaporator and undesirably high gas temperatures entering the convection surface. The temperature of the superheated steam increases and to maintain the preset constant temperatures of the live steam, the mass flow of spray water to the attemperators must be increased. For operational purposes it is convenient to determine some reference temperature. For example, the flue gas temperature leaving the primary superheater commences sootblowing when it reaches a certain value, with allowance being made for boiler loading. In some cases, experienced operators can make judgments on slagging and fouling conditions based on operating conditions, but these secondary indications may be misleading. For example, the furnace can be slagged, causing undesirably high gas temperatures entering the convection surface. However, the steam temperatures and spray attemperation may be normal if the convection surfaces are also fouled. The alternative to blowing at preset times has little to commend it except convenience.

Most furnace-wall sootblowers are typically operated between once a day and three times a shift. The latter frequency of use is perhaps surprising but by no means uncommon, and arises from a need to maximize the absorption of heat by the furnace waterwalls to prevent excessive superheater and, sometimes, reheater steam temperatures.

The computer based boiler performance system, presented in this paper, has been developed to provide a direct and quantitative assessment of furnace and convective surface cleanliness. Measurements of temperature, pressure, flow, and gas analysis data are used to perform a heat transfer analysis in the furnace and convective pass on a bank by bank basis. With a quantitative indication of surface cleanliness, selective sootblowing can be directed at the specific problem area. Sootblower sequencing can be optimized based on actual cleaning requirements rather than on fixed time cycles which can waste blowing medium, increase cycle time, and cause erosion by blowing clean tubes. A boiler monitoring system is also incorporated to provide details of changes in boiler efficiency and operating conditions following sootblowing, so that the effects of a particular sootblowing sequence can be analyzed and optimized later.

### Boiler efficiency

Boiler efficiency is calculated in an on-line mode.

Table 1. Slag monitoring system – input data from measurements and results

Input data	Results
Steam mass flow rate $\dot{m}_s$ , t/h	Boiler efficiency $\eta$ , %
Mass flow rate $\dot{m}_{w1}$ of cooling water to the attemperator No.1, t/h	Loss $S_1$ , %
Mass flow rate $\dot{m}_{w2}$ of cooling water to the attemperator No.2, t/h	Loss $S_2$ , %
Mass flow rate of blow-down water $\dot{m}_b$ , t/h	Loss $S_3$ , %
Drum pressure $p_d$ , MPa	Loss $S_4$ , %
Temperature of spray water to the attemperator $T_{ws}$ , °C	Loss $S_5$ , %
Pressure of live steam $p$ , MPa	Ratio of actual air to theoretical air (Excess air number) $\lambda$
Temperature of live steam $T$ , °C	Boiler thermal power $\dot{Q}_n$ , MW
Superheated steam temperatures $T_1, T_2, T_3$ , and $T_4$ , °C	Fuel mass flow rate $\dot{m}_F$ , kg/s
Air temperature $T_a$ , °C	Flue gas flow rate $\dot{m}_g$ , kg/s
Feed water temperature $T_{fvc}$ before economizer, °C	Volumetric flow of flue gas $\dot{V}_g$ , m <sup>3</sup> /s
Feed water temperature $T_{fwh}$ after economizer, °C	Fouling degree of evaporator $\zeta_{ev}$
Flue gas temperature after superheaters $T_{gs}$ , °C	Fouling degree of superheaters $\zeta_{sup}$
Outlet temperature of flue gas $T_{ge}$ , °C	The effectiveness $\psi$ of furnace waterwalls
Relative air humidity, %	
O <sub>2</sub> (oxygen) content in flue gas by volume, %	
Coal caloric value $W_d$ , kJ/kg	
Ash content in fuel by mass, %	
Combustible in pulverized-fuel ash by mass $U$ , %	
CO (carbon oxide) content in flue gas by volume, %	
Combustible amount in slag $c_{sl}$ , %	
Water velocity in two downcomers, m/s	

The boiler operator can observe time changes of the boiler efficiency and change the selected parameters, for example, the mass flow of the air supplied to the boiler furnace to enhance the efficiency.

Two different techniques for determining the thermal efficiency of the boiler were developed. The first is based

on the caloric value of coal and ash amount, and the second on the ultimate analysis of coal on an “as received” basis. The ultimate analysis specifies, on a mass basis, the relative amounts of carbon, sulfur, hydrogen, nitrogen, oxygen, ash, and the relative amounts of moisture.

The thermal efficiency of the boiler is determined using an indirect method

$$\eta = \frac{\dot{Q}_n}{\dot{Q}_h} = \frac{\dot{Q}_h - \dot{Q}_l}{\dot{Q}_h} = 1 - \frac{\dot{Q}_l}{\dot{Q}_h} \quad (1)$$

where the symbols denote:  $\dot{Q}_n$  - useful heat flow transferred to the working fluid (water and steam),  $\dot{Q}_h$  - heat flow entering the boiler with coal and air,  $\dot{Q}_l$  - heat loss (heat flow transferred to the environment). Expression (1) can be transformed into dimensionless form

$$\eta = 1 - \sum_{i=1}^n S_i, \quad (2)$$

where the dimensionless losses  $S_i$  denote:

$S_1$ -dry flue gas loss,  $S_2$ -loss due to CO content in flue gas (unburned gas loss),  $S_3$ -combustible in pulverized-fuel ash,  $S_4$ -combustible in furnace bottom ash,  $S_5$ -radiation and unaccounted loss,  $S_6$ -sensible heat loss in furnace bottom ash.

The input data and the results of boiler calculations are shown in Table 1.

In addition, twenty thermocouples are installed in four tubular type heat flux meters for monitoring outer and inner scale deposits at waterwalls (Taler et al., 2005). These meters were placed at four different elevations along the height of the combustion chamber. The flux meters are used to measure local slag deposits.

#### Fuel mass flow rate at steady-state conditions

Based on the boiler efficiency evaluated in the on-line mode, a coal mass flow rate will be determined from the definition of the boiler thermal efficiency (Fig. 1)

$$\eta = \frac{\dot{Q}_n}{\dot{Q}_h} = \frac{[(\dot{m}_s - \dot{m}_{w1} - \dot{m}_{w2})(h_s - h_{fwc}) + (\dot{m}_{w1} + \dot{m}_{w2})(h_s - h_{ws}) + \dot{m}_b(h' - h_{fwc})]}{\dot{m}_F H_{LV}} \quad (3)$$

After simple transformations of Eq. (3), we have

$$\dot{m}_F = \frac{(\dot{m}_s - \dot{m}_{w1} - \dot{m}_{w2})(h_s - h_{fwc})}{\eta H_{LV}} + \frac{(\dot{m}_{w1} + \dot{m}_{w2})(h_s - h_{ws}) + \dot{m}_b(h' - h_{fwc})}{\eta H_{LV}} \quad (4)$$

The symbols:  $h_{fwc}$ ,  $h'$ ,  $h_b$ ,  $h_{fwh}$ ,  $h_{ws}$ ,  $h_s$  in equations (3) and (4) denote enthalpy of: feed-water, saturated steam at drum pressure, blow-down water, feed-water after the economizer, spray-water in attemperators, and live steam at outlet of the boiler, respectively (Fig. 1).

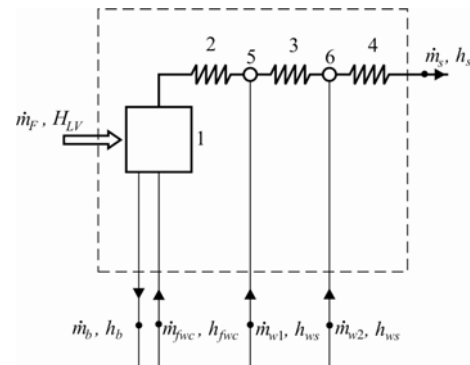


Fig. 1 Control volume for mass and energy balance of a boiler; 1- boiler, 2- 1<sup>st</sup> stage superheater, 3- 2<sup>nd</sup> stage superheater, 4- final superheater, 5- 1<sup>st</sup> stage superheater spray, 6- 2<sup>nd</sup> stage superheater spray

Calculating the ratio of actual air flow to theoretical air flow,  $\lambda$ , from the expression  $\lambda = 21/(21 - O_2)$ , the mass and volumetric flows of humid flue gas are calculated. Equation (4) is valid only for steady-state conditions. The fuel mass flow rate under variable boiler load will be determined from mass and energy balances for the evaporator.

#### Slagging of furnace waterwalls and fouling of superheaters

Deposits are formed on the furnace waterwalls and superheater surfaces if the ash in the flue gas is at a temperature above its melting point. A deposit is usually formed if the flue gas temperature is over 1200°C. The decreased heat absorption due to the build up of deposits can be detected by calculating the following fouling degrees in the on-line mode:

$$\zeta_{ev} = \frac{\dot{Q}_{ev}}{\dot{Q}_{ev}^0(\dot{m}_s)} \quad (5)$$

$$\zeta_{sup} = \frac{\dot{Q}_{sup}}{\dot{Q}_{sup}^0(\dot{m}_s)} \quad (6)$$

The symbols  $\dot{Q}_{ev}^0(\dot{m}_s)$  and  $\dot{Q}_{sup}^0(\dot{m}_s)$  stand for heat flow rates absorbed by the clean evaporator and clean superheaters, respectively. The heat flow rates,  $\dot{Q}_{ev}$  and  $\dot{Q}_{sup}$ , are determined using the measured data from the following expressions (Fig. 2)

$$\dot{Q}_{ev} = (\dot{m}_s - \dot{m}_{w1} - \dot{m}_{w2})h''(p_d) + \dot{m}_b h'(p_d) - \dot{m}_{fw} h_{fwh} \quad (7)$$

$$\dot{Q}_{sup} = (\dot{m}_s - \dot{m}_{w1} - \dot{m}_{w2})[h_1 - h'(p_d)] + (\dot{m}_s - \dot{m}_{w2})(h_3 - h_2) + \dot{m}_s (h_s - h_4) \quad (8)$$

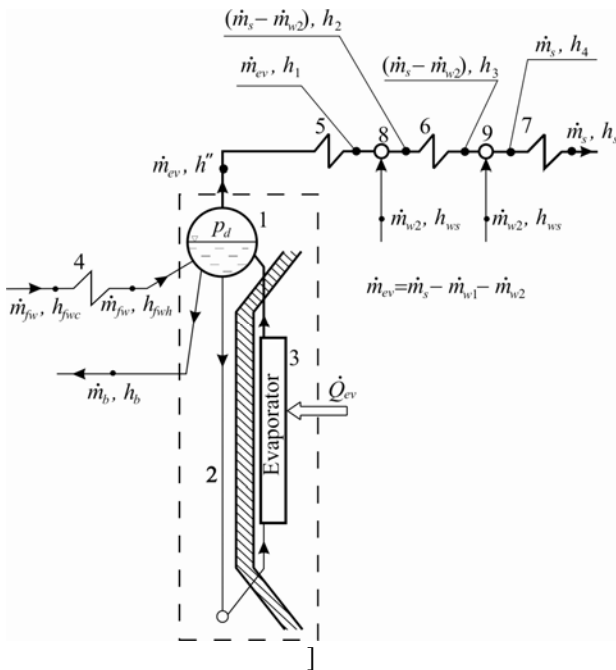


Fig. 2 Control volume for mass and energy balance of boiler evaporator: 1– drum, 2 – downcomers, 3 – evaporator, 4 – economizer, 5 – 1<sup>st</sup> stage superheater, 6 – 2<sup>nd</sup> stage superheater, 7 – final superheater, 8 – 1<sup>st</sup> stage superheater spray, 9 – 2<sup>nd</sup> stage superheater spray

The existing sootblower system is traditionally activated in response to an increase in flue gas temperature  $T_{gs}$  after the steam superheaters, as noted by the operator. This kind of sootblower operation can result in blowing when it is not necessary, which wastes blowing water or steam and can erode tubes. On the other hand, based on the measured temperature

$T_{gs}$ , the temperature of the flue gas  $T'_{fe}$  at the furnace outlet can be calculated and compared to the flue gas temperature  $T_{fe}$  obtained from the calculations of the combustion chamber.

The temperature  $T'_{fe}$  of the flue gas exiting the furnace is given by

$$T'_{fe} = t_{gs} + \frac{\dot{Q}_{sup}}{\dot{m}_g c_{p,g} \Big|_{t_{gs}}^{t'_{fe}}} + 273.15 \quad (9)$$

where the mean specific heat capacity of the flue gas is expressed as

$$c_{p,g} \Big|_{t_{gs}}^{t'_{fe}} = \frac{c_{p,g} \Big|_0^{t'_{fe}} t'_{fe} - c_{p,g} \Big|_0^{t_{gs}} t_{gs}}{t'_{fe} - t_{gs}} \quad (10)$$

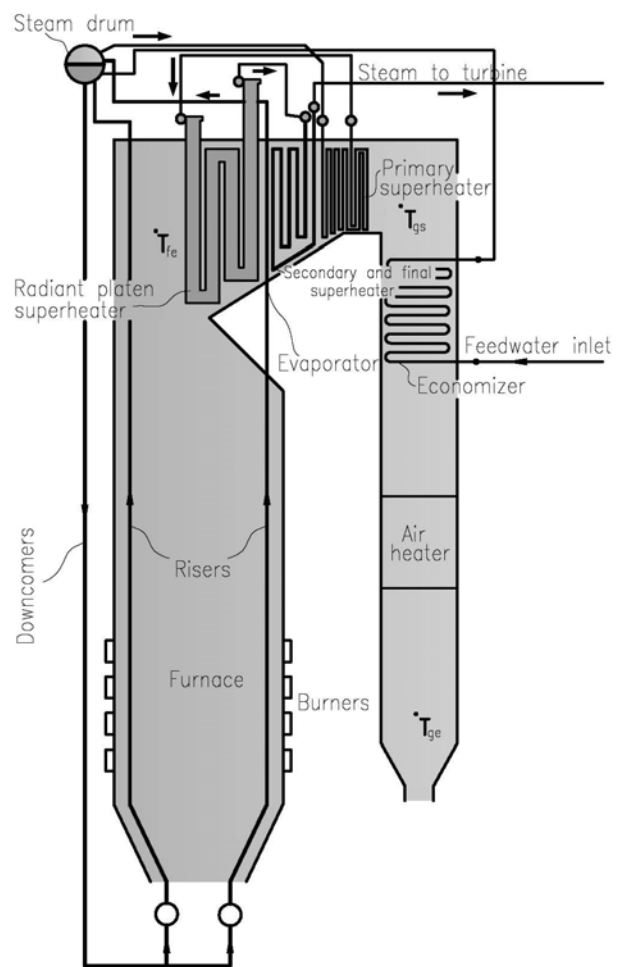


Fig. 3 50 MW coal-fired utility boilers with steam flow rate of  $210 \times 10^3$  kg/h;  $T_{fe}$ ,  $T_{gs}$ , and  $T_{ge}$  denote flue gas temperatures at the furnace exit, after the superheaters and after the air heater

The temperatures  $T_{fe}$  and  $T'_{fe}$  should be equal if the measurements and calculation methods are accurate.

### Mass flow rate of live steam and furnace waterwall effectiveness at steady-state conditions

The mass flow rate of live steam is determined in the on-line mode from mass and energy balance equations (Fig. 2):

$$\dot{m}_{fw} = \dot{m}_s - \dot{m}_{w1} - \dot{m}_{w2} + \dot{m}_b \quad (11)$$

$$\begin{aligned} \dot{m}_{fw} h_{fw} &= \dot{m}_b h'(p_d) + \\ &+ (\dot{m}_s - \dot{m}_{w1} - \dot{m}_{w2}) h''(p_d) + \dot{Q}_{ev} \end{aligned} \quad (12)$$

The substitution of Eq. (11) into Eq. (12) and subsequent transformation gives

$$\dot{m}_s = \frac{\dot{Q}_{ev}}{h''(p_d) - h_{fw}} - \dot{m}_b \frac{h'(p_d) - h_{fw}}{h''(p_d) - h_{fw}} + \dot{m}_{w1} + \dot{m}_{w2} \quad (13)$$

where  $\dot{Q}_{ev}$  denotes rate of heat transferred by radiation and convection from combustion chamber to the surrounding waterwalls. Heat transfer rate  $\dot{Q}_{ev}$  can be calculated from the expression

$$\dot{Q}_{ev} = \dot{Q} - \dot{m}_g \cdot c_{p,g} \Big|_0^{t_{ad}} \cdot t_{fe} \quad (14)$$

where  $\dot{Q}$  is the heat transfer rate entering combustion chamber with coal and air given by

$$\dot{Q} = \dot{m}_g \cdot c_{p,g} \Big|_0^{t_{ad}} \cdot t_{ad} \quad (15)$$

The adiabatic temperature of combustion  $t_{ad}$  expressed in °C is given by

$$t_{ad} = \frac{\dot{m}_F (H_{LV} + h_F) + \dot{m}_a \cdot c_{p,a} \Big|_0^{t_a}}{\dot{m}_g \cdot c_{p,g} \Big|_0^{t_{ad}}} \cdot t_a \quad (16)$$

The well stirred boiler furnace model is used to determine the flue gas temperature exiting the furnace. The rate of heat transfer  $\dot{Q}_r$  transferred by radiation to the water-walls with the surface area  $A_w$  and temperature  $T_w$  can be calculated from the following expression

$$\dot{Q}_r = \sigma \varepsilon_f \psi A_w T_{fl}^4 \quad (17)$$

where  $\sigma = 5.67 \cdot 10^{-8}$  W/(m<sup>2</sup>K<sup>4</sup>) is the Stefan-Boltzmann constant. Taking into account that  $\dot{Q}_{ev} = \dot{Q}_r$  and substituting Eqs (15) and (17) into Eq. (14) gives

$$\frac{T_{fe}}{T_{ad}} = 1 - \frac{\varepsilon_f}{Bo} \left( \frac{T_{fl}}{T_{ad}} \right)^4 \quad (18)$$

where  $Bo$  is the Boltzmann number defined as

$$Bo = \frac{\dot{m}_g \cdot \bar{c}_{p,g}}{\sigma \cdot \psi \cdot A_w \cdot T_{ad}^3} \quad (19)$$

The mean specific heat  $\bar{c}_{p,g}$  over the temperature range [ $t_{fe}$ ,  $t_{ad}$ ] is

$$\bar{c}_{p,g} = \frac{c_{p,g} \Big|_0^{t_{ad}} \cdot t_{ad} - c_{p,g} \Big|_0^{t_{fe}} \cdot t_{fe}}{t_{ad} - t_{fe}} \quad (20)$$

Based on extensive experimental results, the modified relation (18) is used for the outlet flue gas temperature  $T_{fe}/T_{ad}$  (Kuznetsov et al., 1973 and Blokh 1988):

$$\frac{T_{fe}}{T_{ad}} = \frac{1}{M \left( \frac{\varepsilon_f}{Bo} \right)^{0.6} + 1} \quad (21)$$

where  $M$  is a parameter accounting for the kind of fuel (coal, oil or gas) and burners location.

The emissivity of the combustion chamber is given by

$$\varepsilon_f = \frac{\varepsilon_{fl}}{\varepsilon_{fl} + (1 - \varepsilon_{fl}) \psi} \quad (22)$$

where  $\varepsilon_{fl}$  is the flame emissivity and  $\psi$  is the effectiveness of the combustion chamber waterwalls defined as the ratio of the absorbed to incident heat flux.

The waterwall effectiveness  $\psi$  is estimated in the on-line mode from the following nonlinear equation

$$\dot{m}_s^m = \dot{m}_s^c (\psi) \quad (23)$$

where  $\dot{m}_s^m$  and  $\dot{m}_s^c$  is measured and calculated steam mass flow rate, respectively. The mass flow rate  $\dot{m}_s^c$  is calculated using Eq.(13) as a function of the waterwall effectiveness  $\psi$ . The symbol  $\dot{m}_s^m$  stands for measured flow rate with the orifice plate at the outlet of the boiler.

### Fuel mass flow rate at transient conditions

An expression for the steam mass flow from the boiler evaporator will be derived from the conservation equations of mass and energy. The entire evaporator is represented by one control volume by assuming that water and steam are well mixed and remain at one pressure and temperature during a transient. The conservation equations of mass and energy are applied to obtain (Fig.2)

$$\frac{d(V' \rho' + V'' \rho'')}{d\tau} = \dot{m}_{fw} - \dot{m}_{ev} - \dot{m}_b \quad (24)$$

$$\frac{d(V' \rho' u' + V'' \rho'' u'' + m_m c_m T_m)}{d\tau} = \dot{m}_{fw} h_{fwh} - \dot{m}_s h'' - \dot{m}_b i' + \dot{Q}_{ev} \quad (25)$$

Combining the conservation equations of mass and energy gives

$$\begin{aligned} \dot{m}_{ev} = & \frac{\rho' - \rho''}{\rho'(h'' - h')} \left\{ \dot{m}_{fw} \left( h_{fw} - \frac{\rho' h' - \rho'' h''}{\rho' - \rho''} \right) - \right. \\ & - \dot{m}_b \frac{\rho''}{\rho' - \rho''} (h'' - h') + \dot{Q}_{ev} - \left[ V' \left( \rho' \frac{dh'}{dp} + \frac{\rho''(h'' - h')}{\rho' - \rho''} \frac{d\rho'}{dp} - 1 \right) + \right. \\ & \left. \left. + V'' \left( \rho'' \frac{dh''}{dp} + \frac{\rho'(h'' - h')}{\rho' - \rho''} \frac{d\rho''}{dp} - 1 \right) + m_m c_m \frac{dT_m}{dp} \right]_{p=p_d} \frac{dp_d}{d\tau} \right\} \quad (26) \end{aligned}$$

The fuel mass flow rate  $\dot{m}_F$  is determined from the condition

$$\dot{m}_s^m(\tau_i) = \dot{m}_s^c(\tau_i), i = 1, \dots, n \quad (27)$$

where  $\dot{m}_s^m$  and  $\dot{m}_s^c$  is measured and calculated steam mass flow rate at time point  $\tau_i$ , respectively. The heat flow rate  $\dot{Q}_{ev}$  in Eq. (26), given by Eq.(14), is a function of fuel mass flow rate  $\dot{m}_F(\tau)$ . The nonlinear Eq. (27) can be solved by the method of interval searching or iteratively, for example, using the bisection algorithm or the Newton-Raphson method. For the steady-state operation of the boiler, the fuel mass flow rates  $\dot{m}_F$  determined from Eqs (4) and (27) should be equal. When boiler heating surfaces are clean, the consumption of fuel is smaller.

## RESULTS

The computer-based on-line system for monitoring boiler performance, described above, has been installed on a power boiler of  $210 \times 10^3$  kg/h capacity. The heat flow rate absorbed by the clean evaporator  $\dot{Q}_{ev}^0(\dot{m}_s)$  and clean superheaters  $\dot{Q}_{sup}^0(\dot{m}_s)$  (Figs 8 and 9) were determined experimentally. The experimental data point were approximated by simple functions and were used for calculating the fouling degrees  $\zeta_{ev}$  and  $\zeta_{sup}$ , which are defined by Eqs (5) and (6). The results are calculated in the on-line mode and presented graphically, enabling selected parameters to be monitored continuously for several hours. Selected results obtained by means of this system are shown in Figs. 4-11.

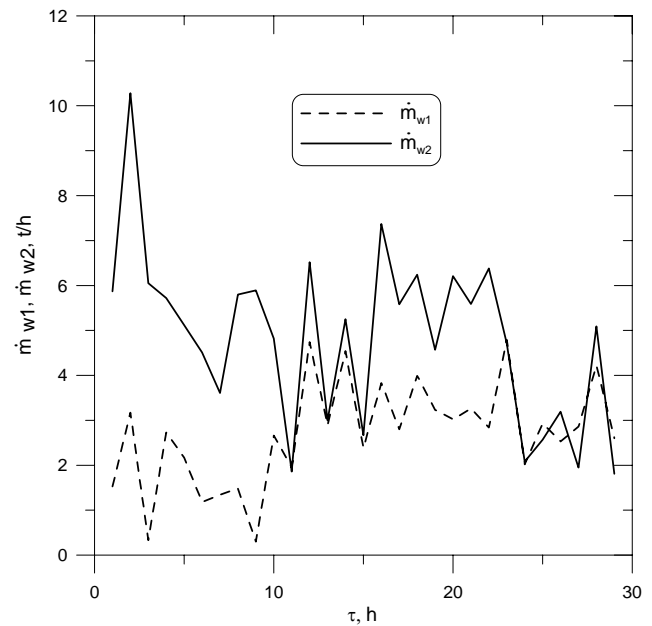


Fig. 4 Mass flow rate of spray water injected into atomizers

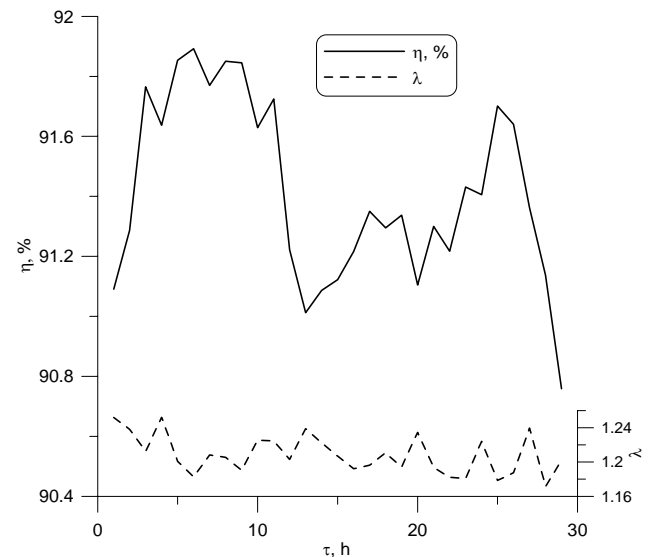


Fig. 5 Excess air number  $\lambda$  and boiler efficiency  $\eta$

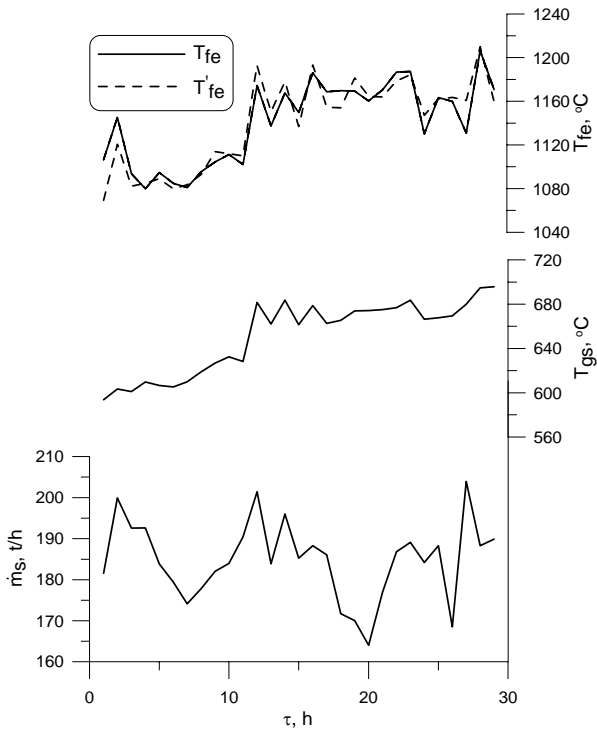


Fig. 6 Flue gas temperatures  $T_{fe}$  and  $T'_{fe}$  at the exit of the furnace, flue gas temperature  $T_{gs}$  after the steam superheaters, and steam mass flow rate  $\dot{m}_s$ :  $T'_{fe}$  - temperature calculated using Eq. (9),  $T_{fe}$  - temperature calculated using Eq. (21)

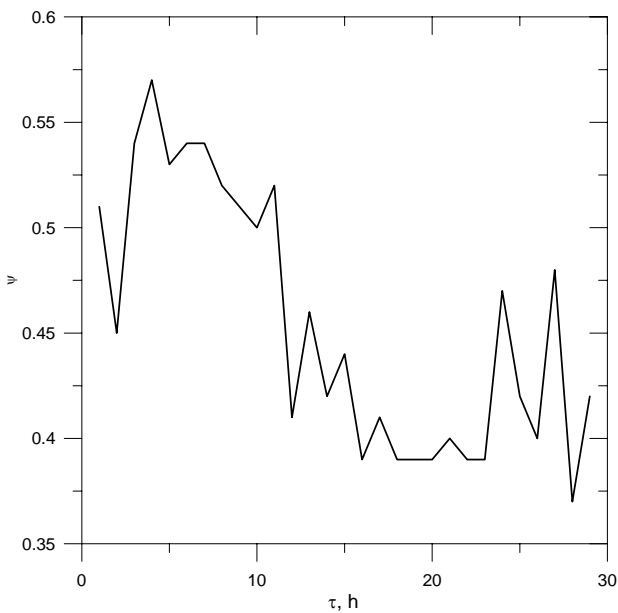


Fig. 7 Waterwall effectiveness  $\psi$  for the boiler furnace

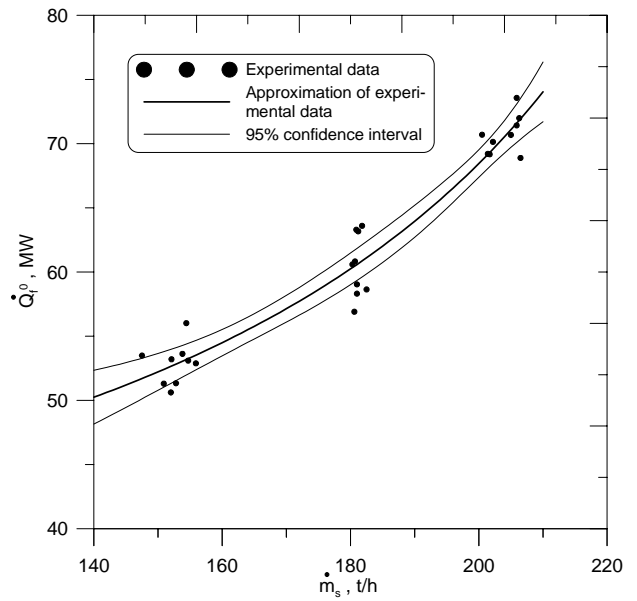


Fig. 8 Heat flow rate  $\dot{Q}_f^0$  absorbed by clean evaporator (furnace waterwalls) versus steam mass flow rate  $\dot{m}_s$  (boiler load)

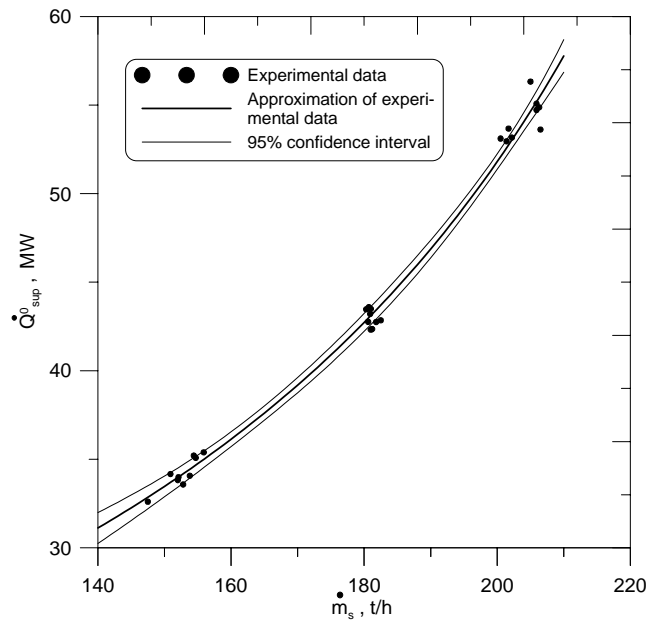


Fig. 9 Heat flow rate  $\dot{Q}_{sup}^0$  absorbed by clean steam superheaters versus steam mass flow rate  $\dot{m}_s$  (boiler load)

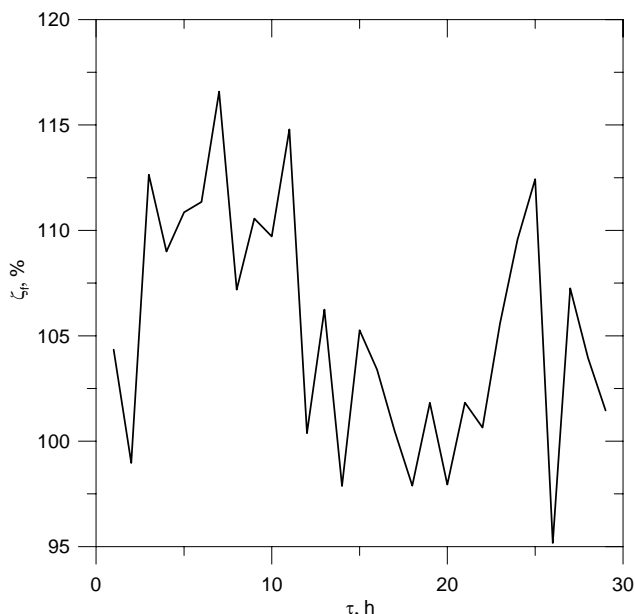


Fig. 10 Degree of slagging  $\zeta_f$  for the furnace

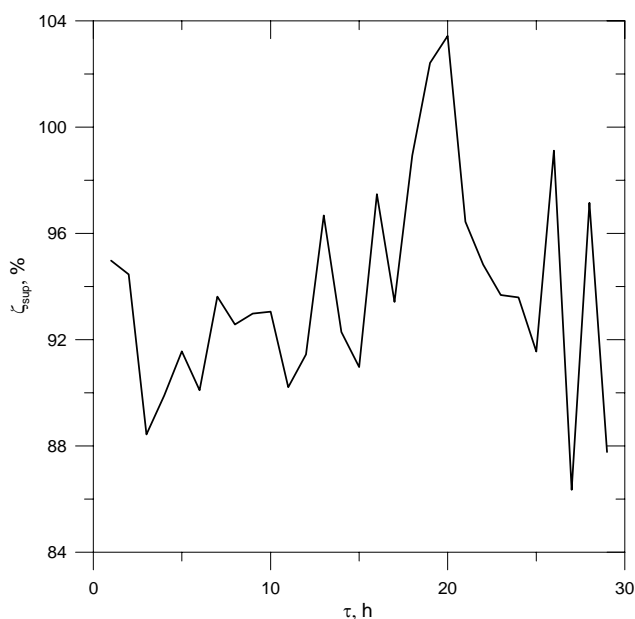


Fig. 11 Degree of fouling  $\zeta_{sup}$  for the steam superheaters

The water sootblowers in the combustion chamber and the steam sootblowers in the superheater region are usually activated once a shift (every 8 hours). For this reason, the boiler fouling analysis is limited to 30h.

Measurements were carried out after the boiler had been cleaned using the sootblowers.

For about the first 10 hours, the heat absorbed by the furnace waterwalls increases (Figs 7 and 10).

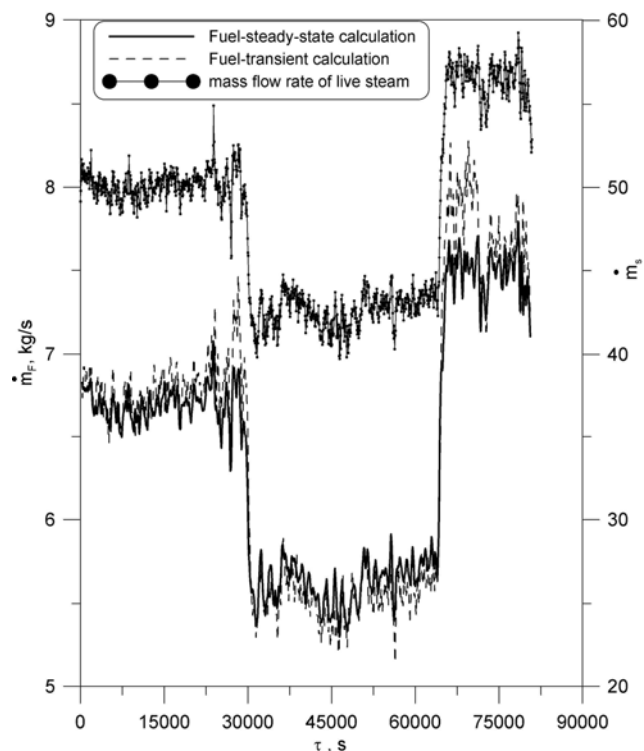


Fig. 12 Comparison of  $\dot{m}_F$  coal flow rate determined from Eq. (4) and (27)

Taking into account that the roughness of the deposition layer is greater than that for clean waterwall tubes, the convective and radiation heat flow rate increases. The convective heat transfer on rough surfaces is better. Also, the radiation heat transfer is enhanced because the emissivity of the rough surface is close to unity. When the deposition layer is thicker, the surface temperature and conductance resistance increases causing the heat flow rate to decrease.

It can be seen from the analysis of the results presented in Figs 4-7 and 10-11 that slag deposits built up on the waterwalls in the furnace. Fouling on the superheater surfaces did not occur. The waterwall effectiveness  $\psi$  determined from Eq. (23) ranges from  $\psi = 0.37$  to  $\psi = 0.57$ . It is worth mentioning that for clean furnace waterwalls of coal fired boilers, the waterwall effectiveness is  $\psi = 0.5$ .

Fig. 12 shows that the mass flow rates of coal  $\dot{m}_F$  calculated from Eqs. (4) and (27) give similar results if the pressure  $p_d$  in the evaporator does not change over time or the pressure variations are small

## CONCLUSIONS

The computer based boiler performance monitoring system has been developed to perform thermal-hydraulic



calculations of the boiler in an on-line mode. Measurements of temperature, pressure, flow, and gas analysis data are used to perform heat transfer analysis in the furnace and convection pass. The state of boiler slagging and fouling, including optimization of sootblowing, can be evaluated from practical plant measurements.

The slag monitoring system can be used to detect the build-up of slag and ash deposits in boiler furnaces and steam superheaters and to guide sootblower operation. In order to raise the boiler efficiency and to reduce fuel cost, the sootblower can be run according to the information obtained from the developed system.

## NOMENCLATURE

$A$  - projected waterwall area,  $m^2$   
 $Bo$  - Boltzmann number, dimensionless  
 $c_p$  - specific heat at constant pressure,  $J/(kg \cdot K)$   
 $h$  - specific enthalpy,  $J/kg$   
 $H_{LV}$  - net calorific value (heating lower value),  $J/kg$   
 $\dot{m}$  - mass flow rate,  $kg/s$   
 $O_2$  - oxygen concentration in flue gas by volume, %  
 $p$  - pressure, Pa  
 $\dot{Q}$  - heat flow rate, W  
 $S$  - heat loss, %  
 $T$  - temperature, K  
 $t$  - temperature,  $^{\circ}C$   
 $u$  - specific internal energy,  $J/kg$   
 $V'$  - volume of saturated water in evaporator,  $m^3$   
 $V''$  - volume of saturated steam in evaporator,  $m^3$

### Greek Letters

$\varepsilon$  - emissivity, dimensionless  
 $\zeta$  - degree of fouling, dimensionless  
 $\eta$  - boiler efficiency, dimensionless  
 $\psi$  - effectiveness of furnace waterwalls, dimensionless  
 $\lambda$  - excess air number, dimensionless  
 $\rho$  - density,  $kg/m^3$   
 $\sigma$  - Stefan - Boltzmann constant,  $\sigma = 5.67 \cdot 10^{-8} \text{ W/m}^2\text{K}^4$   
 $\tau$  - time, s

### Subscripts

a - air  
ad - adiabatic  
b - blowdown water  
d - steam drum  
e - furnace outlet  
ev - evaporator  
f - furnace  
fl - flame

fw - feed water  
fwc - feed water before economizer  
fwh - feed water after economizer  
F - fuel  
g - flue gas  
m - metal  
s - steam  
sl - slag  
sup - superheater  
w - wall  
ws - water spray  
w1 - spray water after the 1<sup>st</sup> stage superheater  
w2 - spray water after the 2<sup>nd</sup> stage superheater

### Superscripts

' - saturated water  
'' - saturated steam  
c - calculated  
m - measured

## REFERENCES

- Blokh, A. G., 1988, *Heat Transfer in Steam Boiler Furnace*, Hemisphere Publishing Corporation, Washington.
- Bergemann, C., 2004, Slag measurement promises better sootblowing, *Modern Power Systems*, Vol.24, No. 2, pp. 34-35.
- Kuznetsov, N. V., Mitor, V. V., Dubovskij, I.E., and Karasina, E.S., 1973, *Standard Methods of Thermal Design for Power Boilers*, Central Boiler and Turbine Institute, Energija, Moscow (in Russian).
- Little, D.J., ed. 1991, *Modern Power Station Practice, Station Operation and Maintenance*, Vol. G, Pergamon Press, Oxford.
- Stultz, S. C., Kitto, J. B., eds., 1992, *Steam/Its Generation and Use*, The Babcock & Wilcox Company, Baberton, Ohio, USA.
- Taler, J., Węglowski, B., Duda, P., Grądziel, S., Sobota, T., Taler, D., and Cebula, A., 2005, Computer monitoring system for boiler performance, *Research Project 6T10/0035/2002C/05798* supported by Ministry of Higher Education and Science and Power Plant Skawina, Cracow, Poland.
- Taler J., and Taler, D., 2007, Tubular type heat flux meter for monitoring internal scale deposits in large steam boilers, *Heat Transfer Engineering*, Vol. 28, No. 3, pp. 230-239.
- Taler, J., 2007, Determination of local heat transfer coefficient from the solution of the inverse heat conduction problem, *Forschung im Ingenieurwesen (Engineering Research)*, Vol.71, pp.69-78.